Molecular Crystals and Liquid Crystals Science and Technology. Section A. Molecular Crystals and Liquid Crystals
Publication details, including instructions for authors and subscription information:
http://www.tandfonline.com/loi/gmcl19

Phase Diagram of n-Tricosane and n-Pentacosane Mixtures

B. Jouti [a], E. Provost [a], D. Petitjean [a], M. Bouroukba [a] & M. Dirand [a]

[a] Laboratoire de Thermodynamique Chimique et Appliquée-Ecole Nationale Supérieure des Industries, Chimiques.1, rue Grandville-BP, 451-F54001, NANCY Cédex, France

Version of record first published: 24 Sep 2006.

To cite this article: B. Jouti , E. Provost , D. Petitjean , M. Bouroukba & M. Dirand (1996): Phase Diagram of n-Tricosane and n-Pentacosane Mixtures, Molecular Crystals and Liquid Crystals Science and Technology. Section A. Molecular Crystals and Liquid Crystals, 287:1, 275-283

To link to this article: http://dx.doi.org/10.1080/10587259608038764

Mol. Cryst. Liq. Cryst., 1996, Vol. 287, pp. 275–283
Reprints available directly from the publisher
Photocopying permitted by license only

Phase Diagram of *n*-Tricosane and *n*-Pentacosane Mixtures

B. JOUTI, E. PROVOST, D. PETITJEAN, M. BOUROUKBA and M. DIRAND

Laboratoire de Thermodynamique Chimique et Appliquée-Ecole Nationale Supérieure des Industries Chimiques. 1, rue Grandville – BP 451 – F54001 NANCY Cédex, France

(Received in final form December 29, 1995)

The phase diagram of the mixtures n-$C_{23}H_{48}$:n-$C_{25}H_{52}$ has been established by joint calorimetric and structural analyses. This study indicates the existence of nine solid single-phase domains of equilibrium: four terminal solid solutions, denoted $\beta_0(C_{23})$, $\beta'_0(C_{23})$, $\beta'_0(C_{25})$ and $\beta_0(C_{25})$ with the *n*-tricosane and *n*-pentacosane structures, three orthorhombic intermediate solid phases, called β''_1, β'_1 and β''_2 (β''_1 and β''_2 on both sides of β'_1 are isostructural), with increasing temperature, two total miscibility fields : β, with the orthorhombic structure Fmmm, above the intermediate solid solution regions (a second order transition which is characterized by the Rotator RI state is observed in this phase) and below the solidus line α-RII with the rhombohedral structure $R\bar{3}m$. These results complete the literature diagrams which only presented two solid single-phase domains.

Keywords: n-Tricosane, n-Pentacosane, binary mixtures, phase diagram, intermediate solid phases, rotator phases.

1. INTRODUCTION

Earlier we have determined the structural evolutions of *n*-tricosane (n-$C_{23}H_{48}$) and *n*-pentacosane (n-$C_{25}H_{52}$) mixtures at 293 K[1]. This study showed the existence of six orthorhombic solid solutions when the molar concentration in *n*-pentacosane increases: three terminal solid solutions, denoted $\beta_0(C_{23})$, $\beta'_0(C_{23})$ and $\beta_0(C_{25})$ isostructural with the *n*-tricosane and *n*-pentacosane structures respectively, and three intermediate phases, called β''_1, β'_1 and β''_2: the two phases β''_1 and β''_2 on both sides of β'_1 are isostructural. The molar concentration ranges of single and two-phase domains had been defined from 0% to 100% in *n*-pentacosane[1]. The orthorhombic structures of the intermediate solid phases are also observed in other binary systems: *n*-docosane (n-$C_{22}H_{46}$):*n*-tetracosane (n-$C_{24}H_{50}$)[2,3], *n*-tetracosane (n-$C_{24}H_{50}$):*n*-hexacosane (n-$C_{26}H_{54}$)[4], *n*-docosane (n-$C_{22}H_{46}$): *n*-tricosane (n-$C_{23}H_{48}$)[5], *n*-tricosane (n-$C_{23}H_{48}$):*n*-tetracosane (n-$C_{24}H_{50}$)[6] and *n*-heneicosane (n-$C_{21}H_{44}$):*n*-tricosane (n-$C_{23}H_{48}$)[7]. Dirand et al.[8] have generalized the thermodynamic and structural behavior of consecutive *n*-alkanes (hereafter called C_n) binary mixtures [even:even-numbered, even:odd-numbered and odd:odd-numbered ($19 < n < 27$)] and they have established the sequences of solid phase appearance when the concentration and the

temperature vary. Our purpose is to establish the phase diagram of the *n*-tricosane (C_{23}) and *n*-pentacosane (C_{25}) mixtures to complete those of the literature[9-13].

2. EXPERIMENTAL METHODS

The two-alkanes (C_{23} and C_{25}) were purchased from the Aldrich Chemical Company: their purity grade is 99 mole per cent as determined by gas chromatography and mass spectrometry analyses. The samples were prepared by weighing together the solid components, melting and thoroughly mixing. Then, the homogeneous liquid solution was quenched in a crystallizing dish maintained at a very low temperature in a Dewar vessel with liquid air. Such rapid cooling ensured a uniform steric concentration in the solid.

The study of the phase diagram has been carried out on twenty six mixtures by combined calorimetric and structural methods.

The differential thermal analyses (DTA) were performed using a SETARAM DSC 111 calorimeter of the Tian Calvet type[14]. The samples were heated from 286 K to above the liquidus point at a rate of 0.5 K min^{-1}. The temperatures of transition peaks are determined with a precision of ± 0.5K. The X-ray diffraction experiments were carried out on powder samples using $\lambda K\alpha$ copper radiation. The X-ray diffractometer (CGR theta 60) analyses were performed at different temperatures with the help of a heated sample holder. Heating or cooling of this sample holder is based on the Peltier effect with a precision of the sample temperature within ± 0.2K around the set point. The focused monochromatic beam was obtained with a filament intensity of 10 mA at 48 kV and the line positions were measured with an accuracy of 0.05° for each value of Bragg angle; the calibration was done with pure aluminium as standard.

On the one hand the peaks, observed on the D.T.A. curves (Fig. 1), showed solid-solid transitions and melting points of the mixtures and indicated the temperature domains of these transformations. On the other hand, these ranges were explored by X-ray diffraction analysis (Fig. 2–3) to characterize the structural evolutions in the course of these solid-solid transitions and to confirm the temperatures of transition start and end. All the experiments have been carried out with increasing temperature at equilibrium state.

3. EXPERIMENTAL RESULTS

3.1. Structural evolutions

The two terminal solid solutions undergo the same solid-solid transitions, as the pure C_{23} and C_{25}. These transformations have been described by many authors[3,4,6,15-32] with the following sequence when the temperature increases:

$$\beta_0(C_{23} \text{ or } C_{25}) \rightarrow \beta'_0(C_{23} \text{ or } C_{25}) \rightarrow \beta\text{-(RI)} \rightarrow \alpha\text{-RII}$$
$$\text{(transition } \delta\text{)}$$

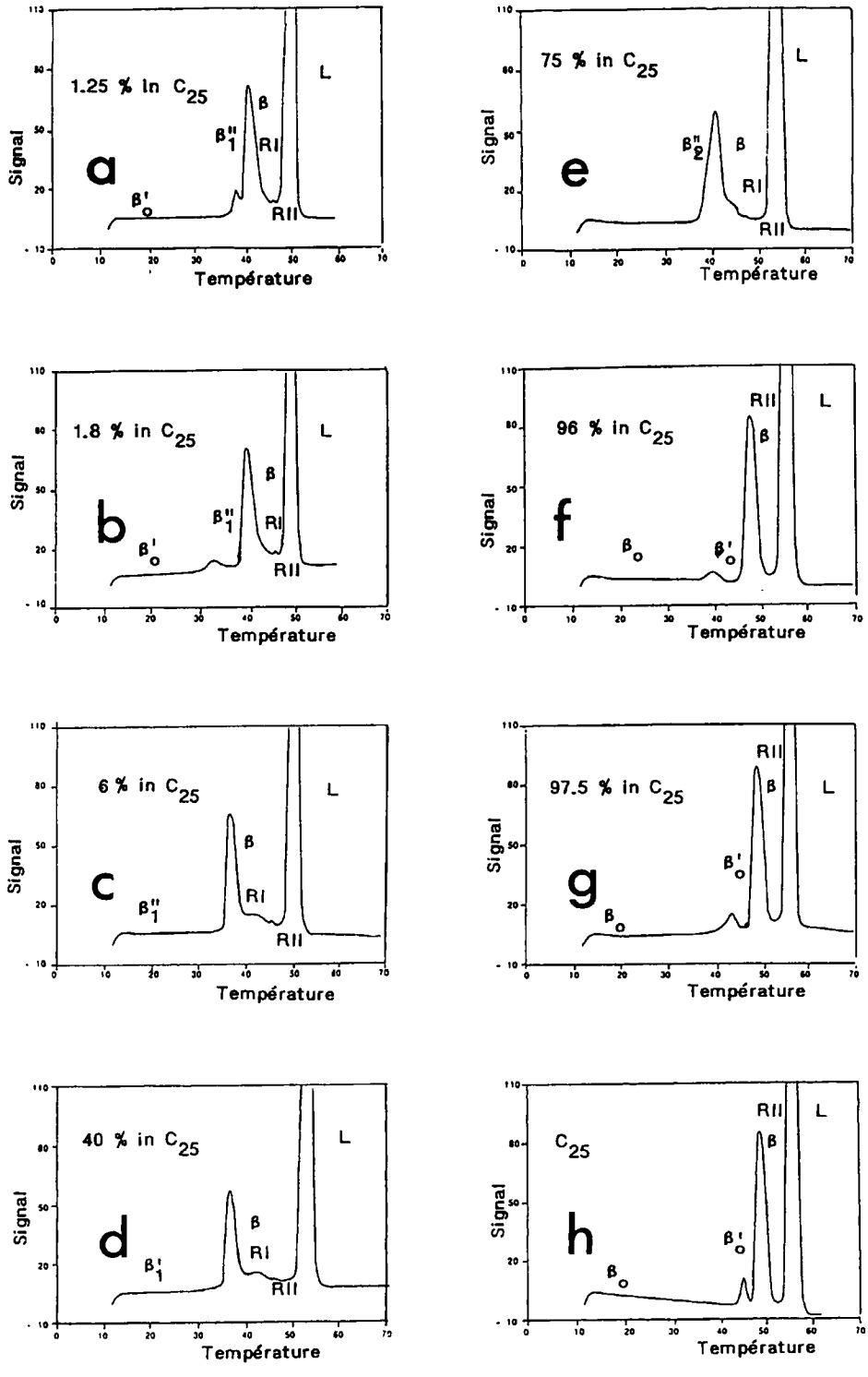

FIGURE 1 Curves of Differential Thermal Analyses (D.T.A.) carried out on mixtures C_{23}:C_{25} at different molar pourcentage in C_{25}: the temperatures are expressed in degree Celsius.

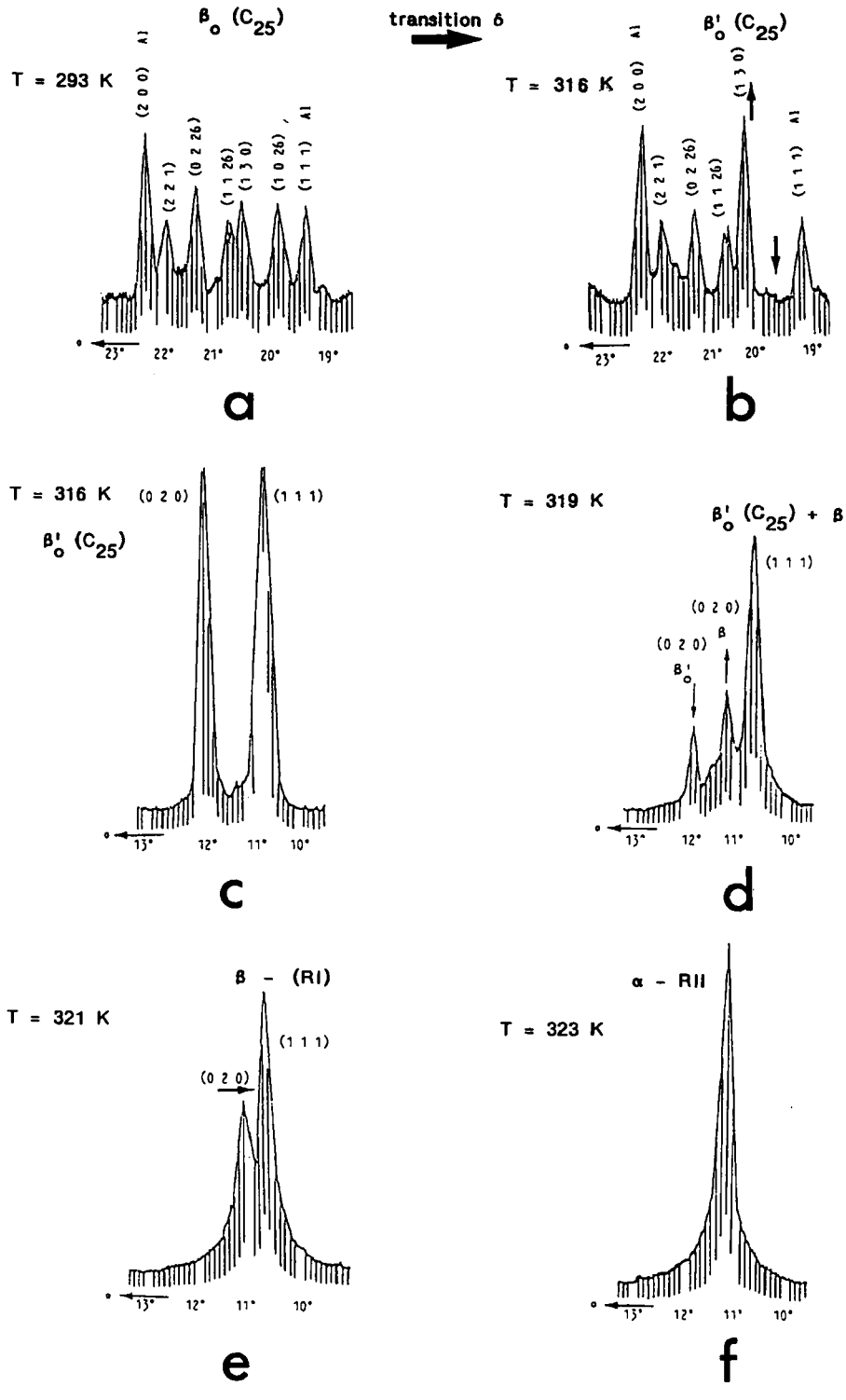

FIGURE 2 Evolution of the X-ray diffractograms from the terminal solid solution $\beta_0(C_{25})$ with 97.5 mol.% of C_{25} at different temperatures, using copper radiation ($\lambda K\alpha$).

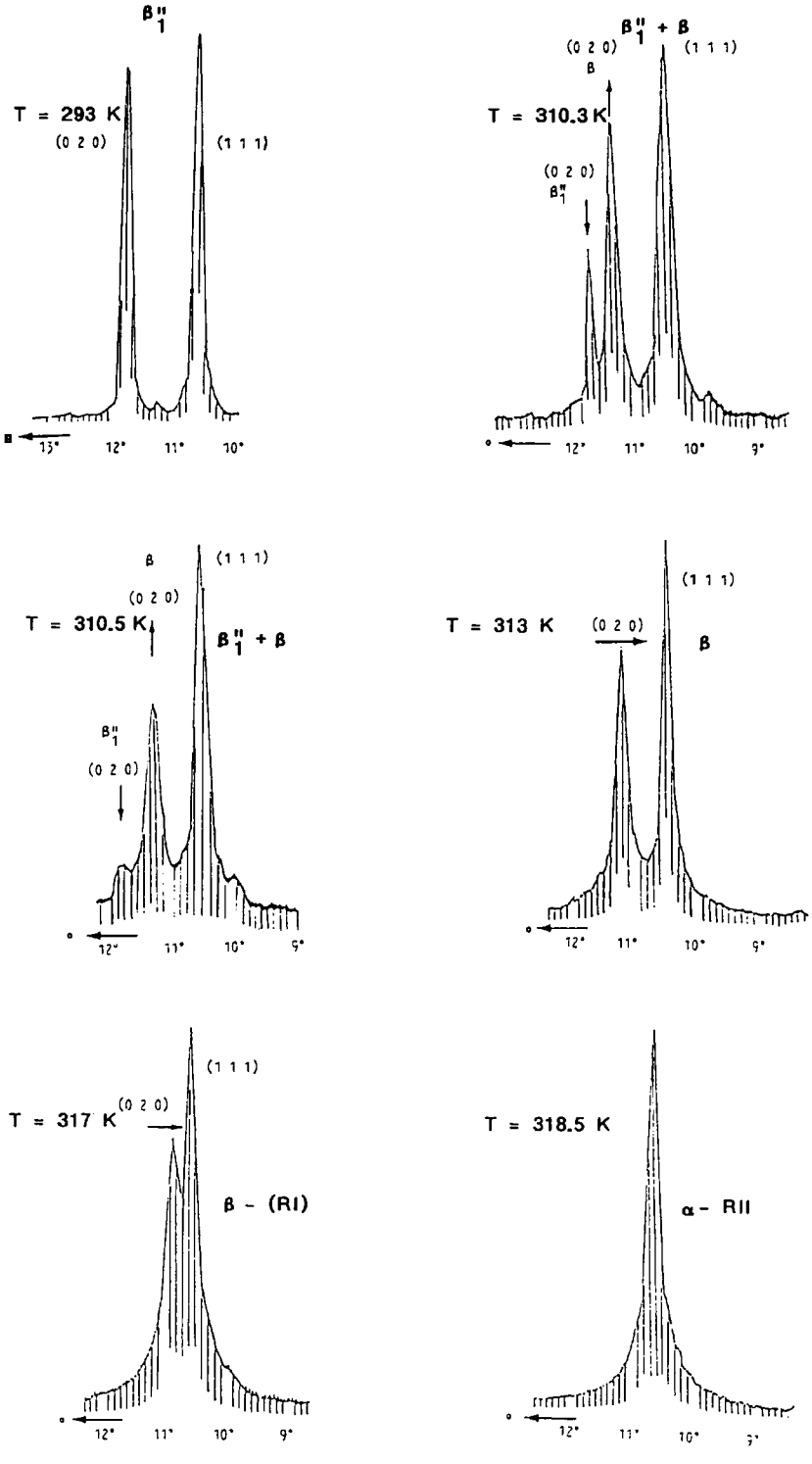

FIGURE 3 Evolution of the X-ray diffractograms from the orthorhombic intermediate phase β_1'' with 4 mol.% of C_{25} (λCuKα).

Notations

$\beta_0(C_{23}$ or $C_{25})$: orthorhombic structure with the space group Pbcm[33]
$\beta'_0(C_{23}$ or $C_{25})$:orthorhombic structure which appears above the transition δ[34]
β:orthorhombic structure with the space group Fmmm[19]

Rotator states

β-RI:Rotator state of the phase β (Fmmm)
α-RII:Rotator phase of rhombohedral structure with the space group $R\bar{3}m$[19]

Figure 2 illustrates the X-ray diffraction spectra evolutions of the terminal solid solution $\beta_0(C_{25})$ with increasing temperature:

i) the transition $\delta(\beta_0(C_{25}) \rightarrow \beta'_0(C_{25}))$ is characterized particularly by (Fig.2a–2b):
   - the disappearance of the line(1 0 26), $\theta = 19,°7$ (λCu Kα)
   - the intensity increase of the peak (1 3 0), $\theta = 20,°4$(λCu Kα)

ii) the occurence of the phase β(Fmmm) is accompanied by:
   - the disappearance of all the diffraction peaks whose indices (h k l) do not have the same parity.
   - an important shift of the diffraction (0 2 0) which corresponds to a considerable increase in the unit cell base area (a,b) (Fig. 2d).

iii) in the Rotator state RI of the phase β (Fmmm), the line (0 2 0) moves progressively to the diffraction peak (1 1 1) with increasing temperature (Fig. 2e).

iv) next, when the two lines (0 2 0) and (1 1 1) coincide (Fig. 2 f), the subcell is hexagonal ($b/a = \sqrt{3}$) and that corresponds to the appearance of the rhombohedral Rotator phase α-RII (R $\bar{3}$ m).

In the single phase domains, the diffraction intensities do not vary; In two-phase regions, the relative intensities of characteristic diffraction lines of each phase evolve (appearance, disappearance or variation Fig. 2b–2d).

As in the systems (C_{22}:C_{24}[3,15], C_{24}:C_{26}[4,32], C_{23}:C_{24}[6], C_{22}:C_{23}[5]), when the temperature increases, the solid phase sequence from the orthorhombic intermediate phases β''_1, β'_1 and β''_2 corresponds to the following scheme:

$$-\,T(K)\rightarrow$$

$$\beta''_1,\ \beta'_1 \text{ or } \beta''_2 \rightarrow \beta\text{-(RI)} \rightarrow \alpha\text{-RII} \rightarrow \text{liquid}$$

The structural evolutions (Fig. 3) are identical to those which were observed previously for the terminal solid solutions β_0 (C_{23} or C_{25}) above their transition δ up to their melting points (Fig. 2).

3.2. Differential thermal analyses

The D.T.A. curves for different concentrations are shown in Fig. 1. The solid phase structures were identified by X-ray diffraction analyses on samples from either side of

DTA peaks. The two important enthalpy effects, that are always observed respectively correspond to the appareance of the phase β(Fmmm) and the melting.

The thermal accident sequence from the two terminal solid solutions β_0 (C_{23}) and β_0 (C_{25}) (Fig. 1-f, 1-g, 1-h) is similar to that obtained in pure C_{23} and C_{25} [19,4,32] and in the phase β_0 (C_{23}) of binary systems (C_{23}:C_{22})[5] and (C_{23}:C_{24})[6]. Particularly, the first small peak corresponds to the transition $\delta(\beta_0 \rightarrow \beta'_0)$: its temperature which decreases versus solute concentration (Fig. 1-h, 1-g, 1-f) allows to determine the limit curve of solubility in the terminal solid solutions β_0 (Fig. 4).

The sequence of D.T.A. peaks for the second terminal solid solution β'_0(C_{23}) (Fig. 1-a, 1-b) corresponds to the following transitions:

i) β'_0 (C_{23}) $\rightarrow \beta''_1$: first small peak.
ii) β''_1: $\rightarrow \beta$(Fmmm): second peak which is characterized by an important enthalpy effect.
iii) then, in the Rotator state RI of the phase β (Fmmm), the differential signal does not return to the basis line in a many degree range. Moreover the X-ray diffraction line intensities do not change significantly and we have not observed the appearance of a second phase which characterizes a first-order transition in the binary systems: this structural and thermodynamic behaviour corresponds to a second order transition without any change in phase or concentration.

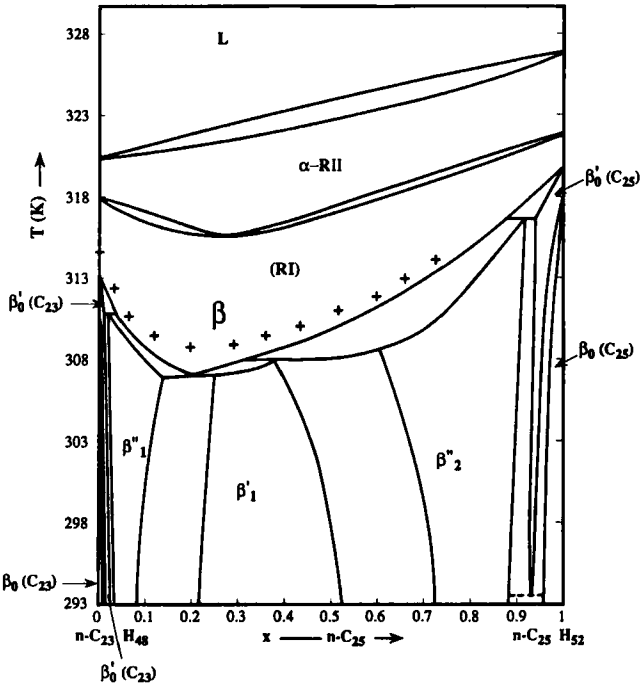

FIGURE 4 Phase diagram of the C_{23}:C_{25} mixtures. The + + + line indicates the beginning temperature of the second-order transition which characterizes the Rotator state RI of the phase β(Fmmm).

iv) next the small peak, just below the important peak of the melting: β-(RI) $\rightarrow \alpha$-RII.

The temperature of the transition $\beta'_0(C_{23}) \rightarrow \beta''_1$ decreases versus the molar concentration in C_{25} (Fig. 1a, 1b). This observation allows the determination of the solubility limit curve of C_{25} in the phase β'_0 (C_{23}) (Fig. 4).

The D.T.A. curves, which have been obtained from intermediate solid solutions β''_1, β'_1 and β''_2 (Fig. 1c, 1d, 1e), are identical to those observed on the terminal solid solutions: however the first small peak is not present.

These joint thermodynamic and structural studies allow the determination of the whole of solid-solid and solid-liquid transition temperatures and to establish the C_{23}:C_{25} phase diagram (Fig. 4), using also the results that we have earlier obtained at 293 K[1].

4. CONCLUSION

The calorimetric and X-ray analyses of the binary mixtures C_{23}:C_{25} indicate the existence of nine solid single-phase domains of equilibrium:

i) four terminal solid solutions:

β_0 (C_{23}) and $\beta_0(C_{25})$, orthorhombic Pbcm
β'_0 (C_{23}) and $\beta'_0(C_{25})$, with the orthorhombic structure of C_{23} and C_{25}, observed above the transition δ.

The β'_0 (C_{25}) undergoes an eutectoid decomposition above 293 K:

$$\beta'_0(C_{25}) \rightarrow \beta_0(C_{25}) + \beta''_2 \text{ (Fig. 4).}$$

ii) three intermediate solid solutions β''_1, β'_1, β''_2, orthorhombic: the phases β''_1 and β''_2 are isostructural[1].

iii) with increasing temperature, two total miscibility fields:

- β, orthorhombic Fmmm: a second order transition which is characterized by the Rotator RI state is observed in this phase.
- α-RII, rhombohedral $R\bar{3}m$.

Our results complete the literature diagrams[9-13] which only presented two solid single-phase domains. They also confirm the generalization of thermodynamic and structural behavior in the binary mixtures of consecutive *n*-alkanes which has been established by DIRAND *et al.*[8].

References

1. B. Jouti, J. B. Bourdet, M. Bouroukba, M. Dirand, *Mol. Cryst. Liq. Cryst.*, **270**, 159 (1995).
2. N. Hasnaoui, J. Dellacherie, L. Schuffenecker, M. Dirand, D. Balesdent, *J. Chim. Phys.*, **85** (6), 153 (1988).
3. Z. Achour, J. B. Bourdet, M. Bouroukba, M. Dirand, *Thermochim. Acta.*, **204**, 187 (1992).

4. Z. Achour-Boudjema, J. B. Bourdet, D. Petitjean, M. Dirand, *J. of Mol. Struct.*, **354**, 197 (1995)
5. A. Sabour, *Ph.Thesis INPL-Nancy* (France) (1994).
6. A. Sabour, J. B. Bourdet, M. Bouroukba, M. Dirand, *Thermochim. Acta*, **249**, 269 (1995)
7. B. Jouti, J. B. Bourdet, M. Bouroukba, M. Dirand, *J. of Mol. Struct.*, **356**, 191 (1995).
8. M. Dirand, Z. Achour, B. Jouti, A. Sabour, J. C. Gachon, *Mol. Cryst. Liq. Cryst.*, **270**, 159 (1995).
9. W. M. Mazee, *J. Inst. Petrol.* **35**, 97 (1949).
10. W. M. Mazee, *Analyst. Chem. Acta*, **17**, 97 (1957).
11. W. M. Mazee, *Symp. Adv. Chem. Thermod.*, **B35–B48** (1958).
12. W. M. Mazeem, *Erdol und Kohle.*, **13.2**, 88 (1960).
13. J. J. Retief, D. Wengel, E. G. Boonstra, *J. Appl. Cryst.*, **18**.156 (1985).
14. E. Calvet, H. Prat, *Microcalorimetrie. Applications Physico-Chimie et Biologiques*, Masson, Paris (1956).
15. N. Hasnaoui, J. Dellacherie, L. Schuffenecker, M. Dirand, D. Balesdent, *J. Chim. Phys.*, **85** (6), 675 (1988).
16. J. Doucet, I. Denicolo, A. Craievich, *J. Chem. Phys.*, **75**, 3 1523 (1981).
17. J. Doucet, I. Denicolo, A. Craievich, A. Collet, *J. Chem. Phys.*, **75** (10), 5125 (1981).
18. A. Holz, J. Naghizadeh, D. T. Virgen, *Phys. Rev.*, **B27**, 1 512 (1983).
19. I. Denicolo, J. Doucet, A. F. Craievich, *J. Chem. Phys.*, **78**, 3 1465 (1983).
20. G. Ungar, *J. Phys. Chem.*, **87**, 689 (1983).
21. J. Doucet, I. Denicolo, A. F. Craievich, G. Germain, *J. Chem. Phys.*, **80**, 4 1647 (1984).
22. J. Doucet, A. J. Dianoux, *J. Chem. Phys.*, **81**, 11 5043 (1984).
23. I. Denicolo, A. F. Craievich, J. Doucet, *J. Chem. Phys.*, **80**, 12 6200 (1984).
24. S. K. Filatov, E. N. Kotelnikova, E. A. Alek Sandrova, *Zeitsch fur Krist.*, **172**, 35 (1985).
25. R. S. Cantor, K. A. Dill, *Macromol.* **18**, 1875 (1985).
26. J. P. Ryckaert, M. I. Klein, I. R. Mac Donald, *Phys. Rev. Letters*, **58**, 7 698 (1987).
27. I. A. M. Royaud, P. J. Hendra, W. Maddams, C. Passingham., H. A. Willis, *J. of Mol. Struct.*, **239**, 83 (1990).
28. R. D. Heyding, K. E. Russel, T. L. Varty, D. St Cyr, *Powder Dif.*, **5**, 2 93 (1990).
29. A. Toda, H. Miyaji, Y. Ogawa, K. Takamizawa, *J. of Mat. Sc.*, **26**, 2793 (1991).
30. E. B. Sirota, H. E. King, Jr. D. M. Singer, H. H. Shao, *J. Chem. Phys.*, **98**, 5809 (1993).
31. K. Nozakik, N. Higashitani, T. Yamamoto, T. Hara, *J. Chem. Phys.*, **103** (13), 5762 (1995).
32. Z. Achour-Boudjema, M. Bouroukba, M. Dirand, *Thermo Chim. Acta* (publication in press).
33. A. E. Smith, *J. Chem. Phys.*, **21**, 2229 (1953).
34. R. G. Snyder, A. F. Maroncelli, S. P. Qi, H. L. Strauss, *Science*, **214** (9), 188 (1981).